22

AggieAir: Towards Low-cost Cooperative Multispectral Remote Sensing Using Small Unmanned Aircraft Systems

[a]Haiyang Chao, [a,b]Austin M. Jensen, [a]Yiding Han, [a]YangQuan Chen and [b]Mac McKee
[a]*Center for Self Organizing and Intelligent Systems (CSOIS),Utah State University*
haiyang.chao@aggiemail.usu.edu, yqchen@ieee.org
[b]*Utah Water Research Laboratory (UWRL), Utah State University*
austin.jensen@aggiemail.usu.edu
United States of America

1. Introduction

This chapter focuses on using small low-cost unmanned aircraft systems (UAS) for remote sensing of meteorological and related conditions over agricultural fields or environmentally important land areas. Small UAS, including unmanned aerial vehicle (UAV) and ground devices, have many advantages in remote sensing applications over traditional aircraft- or satellite-based platforms or ground-based probes for many applications. This is because small UAVs are easy to manipulate, cheap to maintain, and remove the need for human pilots to perform tedious or dangerous jobs. Multiple small UAVs can be flown in a group and complete challenging tasks such as real-time mapping of large-scale agriculture areas.

The purpose of remote sensing is to acquire information about the Earth's surface without coming into contact with it. One objective of remote sensing is to characterize the electromagnetic radiation emitted by objects (James, 2006). Typical divisions of the electromagnetic spectrum include the visible light band ($380 - 720nm$), near infrared (NIR) band ($0.72 - 1.30\mu m$), and mid-infrared (MIR) band ($1.30 - 3.00\mu m$). Band-reconfigurable imagers can generate several images from different bands ranging from visible spectra to infra-red or thermal based for various applications. The advantage of an ability to examine different bands is that different combinations of spectral bands can have different purposes. For example, the combination of red-infrared can be used to detect vegetation and camouflage and the combination of red slope can be used to estimate the percent of vegetation cover (Johnson et al., 2004). Different bands of images acquired remotely through UAS could be used in scenarios like water management and irrigation control. In fact, it is difficult to sense and estimate the state of water systems because most water systems are large-scale and need monitoring of many factors including the quality, quantity, and location of water, soil and vegetations. For the mission of accurate sensing of a water system, ground probe stations are expensive to build and can only provide data with very limited sensing range (at specific positions and second level temporal resolution). Satellite photos can cover a large area, but have a low resolution and a slow update rate (30-250 meter or lower spatial resolution and week level temporal resolution). Small UAVs cost less money but can provide more accurate information (meter or centimeter spatial

resolution and hour-level temporal resolution) from low altitudes with less interference from clouds. Small UAVs combined with ground and orbital sensors can even form a multi-scale remote sensing system.

UAVs equipped with imagers have been used in several agricultural remote sensing applications for collecting aerial images. High resolution red-green-blue (RGB) aerial photos can be used to determine the best harvest time of wine grapes [Johnson et al. 2003]. Multispectral images are also shown to be potentially useful for monitoring the ripeness of coffee [Johnson et al. 2004]. Water management is still a new area for UAVs, but it has more exact requirements than other remote sensing applications: real-time management of water systems requires more and more precise information on water, soil and plant conditions, for example, than most surveillance applications. Most current UAV remote sensing applications use large and expensive UAVs with heavy cameras (in the range of a kilogram). Images from reconfigurable bands taken simultaneously can increase the final information content of the imagery and significantly improve the flexibility of the remote sensing process.

Motivated by the above remote sensing problem, AggieAir, a band-configurable small UAS-based remote sensing system has been developed in steps at Center for Self Organizing and Intelligent Systems (CSOIS) together with Utah Water Research Lab (UWRL), Utah State University. The objective of this chapter is to present an overview of the ongoing research on this topic.

The chapter first presents a brief overview of the unmanned aircraft systems focusing on the base of the whole system: autopilots. The common UAS structure is introduced. The hardware and software aspects of the autopilot control system are then explained. Different types of available sensor sets and autopilot control techniques are summarized. Several typical commercial off-the-shelf and open source autopilot packages are compared in detail, including the Kestrel autopilot from Procerus, Piccolo autopilot from CloudCap, and the Paparazzi open source autopilot etc.

The chapter then introduces AggieAir, a small and low-cost UAS for remote sensing. AggieAir comprises of a flying-wing airframe as the test bed, the OSAM-Paparazzi autopilot for autonomous navigation, the Ghost Foto image system for image capture, the Paparazzi ground control station (GCS) for real time monitoring, and the gRAID software for image processing. AggieAir is fully autonomous, easy to manipulate, and independent of a runway. AggieAir can carry embedded cameras with different wavelength bands, which are low-cost but have high spatial resolution. These imagers mounted on UAVs can form a camera array to perform multi-spectral imaging with reconfigurable bands, depending on the objectives of the mission. Developments of essential subsystems, such as the UAV autopilot, imaging payload subsystem, and image processing subsystem, are introduced in detail together with some experimental results to show the orthorectification accuracy.

Several typical example missions together with real UAV flight test results are focused in Sec.3 including land survey, water area survey, riparian applications and remote data collection. Aerial images and stitched maps showed the effectiveness of the whole system. The future direction is more accurate orthorectification method and band-reconfigurable multi-UAV-based cooperative remote sensing for real-time water management and distributed irrigation control.

2. Small UAS Overview

In this paper, the acronym UAV (Unmanned Aerial Vehicle) is used to represent a power-driven, reusable airplane operated without a human pilot on board. The UAS (Unmanned

Aircraft System) is defined as an UAV and its associated elements which may include ground control stations, data communication links, support equipment, payloads, flight termination systems, and launch/recovery equipments (Tarbert et al., 2009). Small UAS (sUAS) could be categorized into five groups based on gross take-off weight by the sUAS aviation rule making committee, as shown in Tab. 1. Group *i* include those constructed in a frangible manner that would minimize injury and damages if there is a collision, compared with group *ii*.

Group	Gross Take-off Weight
i	$\leq$ 4.4 lbs or 2 kgs
ii	$\leq$ 4.4 lbs or 2 kgs
iii	$\leq$ 19.8 lbs or 9 kgs
iv	$\leq$ 55 lbs or 25 kgs
v	lighter than air (LTA) only

Table 1. Small UAS Categories

The topic of small UAS is quite active in the past few years (Chao et al., 2009). A lot of small fixed-wing or rotary-wing UAVs are flying in the air under the guidance from the autopilot systems for different applications like forest first monitoring, coffee field survey, search and rescue, etc. A typical UAS includes:

(1) Autopilot: an autopilot is a MEMS system used to guide the UAV without assistance from human operators, consisting of both hardware and its supporting software. The autopilot is the base for all the other functions of the UAS platform.

(2) Airframe: the airframe is where all the other devices are mounted including the frame body, which could be made from wood, foam or composite materials. The airframe also includes the flight control surfaces, which could be a combination of either aileron/elevator/rudder, or elevator/rudder, or elevons.

(3) Payload: the payload of UAS could be different bands of cameras, or other emission devices like Lidar mostly for intelligence, surveillance, and reconnaissance uses.

(4) Communication system: most UAS have more than one wireless link supported. For example, RC link for safety pilot, wifi link for large data sharing, and wireless serial modem.

(5) Ground control station: ground control station is used for real-time flight status monitoring and flight plan changing.

(6) Launch and recovery devices: some UAS may need special launching devices like a hydraulic launcher or landing devices like a net.

The whole UAS structure is shown in Fig 1. The minimal UAS onboard system requires the airframe for bedding all the devices, the autopilot for sensing and navigation, the basic imaging payload for aerial images, and the communication systems for data link with the ground. The left section concentrates on the autopilot overview since it is the base for the UAS platform and it also needs to provide accurate orientation and position data for each data set the UAS collects.

Autopilot systems are now widely used in modern aircrafts and ships. The objective of UAV autopilot systems is to consistently guide UAVs to follow reference paths, or navigate through some waypoints. A powerful UAV autopilot system can guide UAVs in all stages including

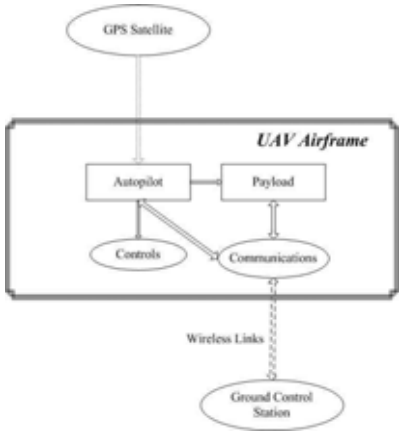

Fig. 1. UAS Structure.

take-off, ascent, descent, trajectory following, and landing. The autopilot needs also to communicate with ground station for control mode switch, to receive broadcast from GPS satellite for position updates and to send out control inputs to the servo motors on UAVs.
An UAV autopilot system is a close-loop control system with two fundamental functions: state estimation and control signal generation based on the reference paths and the current states. The most common state observer is the inertial measurement unit (IMU) including gyros, accelerometers, and magnetic sensors. There are also other attitude determination devices available like infrared or vision based ones. The sensor readings combined with the GPS information can be passed to a filter to generate the estimates of the current states for later control uses. Based on different control strategies, the UAV autopilots can be categorized to PID based autopilots, fuzzy based autopilots, neutral network (NN) based autopilots, etc. A typical off-the-shelf UAV autopilot system comprises of the GPS receiver, the IMU, and the onboard processor (state estimator and flight controller) as illustrated in Fig. 2.

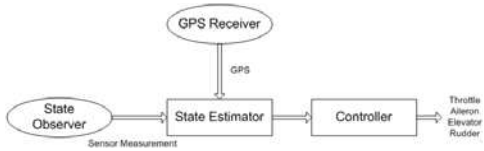

Fig. 2. Functional Structure of the UAV Autopilot.

Due to the limited size and payload of the small UAVs, the physical features like size, weight and power consumption are the primary issues that the autopilot must take into consideration. A good autopilot should be small, light and have a long endurance life. It is not so hard to design the hardware to fulfill the autopilot requirements. The current bottleneck for autopilot systems lies more in the software side.

2.1 Autopilot Hardware

A minimal autopilot system includes sensor packages for state determination and onboard processors for estimation & control uses, and peripheral circuits for servo & modem communications. Due to the physical limitations of small UAVs, the autopilot hardware needs to be of small sizes, light weights and low power consumptions. The accurate flight control of UAVs demands a precise observation of the UAV attitude in the air. Moreover, the sensor packages should also guarantee a good performance, especially in a mobile and temperature-varying environment.

2.1.1 MEMS Inertial Sensors

Inertial sensors are used to measure the 3-D position and attitude information in the inertial frame. The current MEMS technology makes it possible to use tiny and light sensors on small or micro UAVs. Available MEMS inertial sensors include:

(1) GPS receiver: to measure the positions (p_n, p_e, h) and ground velocities (v_n, v_e, v_d).

(2) Rate or gyro: to measure the angular rates (p, q, r).

(3) Acceleration: to measure the accelerations (a_x, a_y, a_z).

(4) Magnetic: to measure the magnetic field for the heading correction (ψ).

(5) Pressure: to measure the air speed (the relative pressure) and the altitude (h).

(6) Ultrasonic sensor or SONAR: to measure the relative height above the ground.

(7) Infrared sensor: to measure the attitude angles (ϕ,θ).

(8) RGB camera or other image sensors: to replace one or several of the above sensors.

GPS plays an indispensable role in the autonomous control of UAVs because it provides an absolute position measurement. A known bounded error between GPS measurement and the real position can be guaranteed as long as there is a valid 3-D lock. For instance, u-blox 5 GPS receiver could achieve a three meter 3-D accuracy (PACC) in the best case for civilian applications in the United States. There are also differential GPS units which could achieve centimeter level accuracy. The disadvantage of GPS is its vulnerability to weather factors and its relatively low updating frequency (commonly 4Hz), which may not be enough for flight control applications.

2.1.2 Possible Sensor Configurations

Given all the above inertial sensors, several sensor combinations could be chosen for different types of UAVs to achieve the basic autonomous waypoints navigation task. Most current outdoor UAVs have GPS receivers onboard to provide the absolute position feedback. The main difference is the attitude measurement solution, which could be inertial measurement unit (IMU), infrared sensor or image sensor etc.

2.1.2.1 Inertial Measurement Unit (IMU)

A typical IMU includes 3-axis gyro rate and acceleration sensors, which could be filtered to generate an estimation of the attitude (ϕ, θ, ψ). A straightforward sensor solution for small UAVs is to use the micro IGS, which can provide a complete set of sensor readings. Microstrain Gx2 is this kind of micro IMU with an update rate up to 100 Hz for inertial sensors. It has 3-axis magnetic, gyro and acceleration sensors (Microstrain Inc., Accessed 2008).

2.1.2.2 Infrared Sensor

Another solution for attitude sensing is using infrared thermopiles. The basic idea of infrared attitude sensor is to measure the heat difference between two sensors on one axis to determine the angle of the UAV because the Earth emits more IR than the sky. Paparazzi Open Source Autopilot group used this kind of infrared sensors as their primary attitude sensor (Paparazzi Forum, Accessed 2008) (Egan, 2006). The infrared sensors can be used for UAV stabilization and RC plane training since it can work as a leveler. However, it is not that accurate for later georeferecing.

2.1.2.3 Vision Sensor

Vision sensor could also be used to estimate the attitude by itself or combined with other inertial measurements (Roberts et al., 2005). The pseudo roll and pitch can be decided from the onboard video or image streams (Damien et al., 2007). Experiments on vision only based navigation and obstacle avoidance have been achieved on small rotary wing UAVs (Calise et al., 2003). In addition, vision based navigation has potentials to replace the GPS in providing position measurements especially in task oriented and feature based applications. Vision based navigation for small fixed wing UAVs is still an undergoing topic and a lot of work are still needed for mature commercial autopilots.

2.2 Autopilot Software

All the inertial measurements from sensors will be sent to the onboard processor for further filter and control processing. Autopilot could subscribe services from the available sensors based on different control objectives.

2.2.1 Autopilot Control Objectives

Most UAVs can be treated as mobile platforms for all kinds of sensors. The basic UAV waypoints tracking task could be decomposed into several subtasks including:

(1) Pitch attitude hold.

(2) Altitude hold.

(3) Speed hold.

(4) Automatic take-off and landing.

(5) Roll-Angle hold.

(6) Turn coordination.

(7) Heading hold.

There are two basic controllers for the UAV flight control: altitude controller, velocity and heading controller. Altitude controller is to drive the UAV to fly at a desired altitude including the landing and take-off stages. The heading and velocity controller is to guide the UAV to fly through the desired waypoints. Most commercial autopilots use PID controllers, and the control parameters could be tuned off-line first and re-tuned during the flight.

2.3 Typical Autopilots for Small UAVs

In this section, several available autopilots, including both commercial and open source ones, are introduced and compared in terms of sensor configurations, state estimations and controller strengths. Most commercial UAV autopilots have sensors, processors and peripheral

circuits integrated into one single board to account for size and weight constraints. The advantage of the open source autopilots is its flexibility in both hardware and software. Researchers can easily modify the autopilot based on their own special requirements.

2.3.1 Procerus Kestrel Autopilot

Procerus Kestrel Autopilot is specially designed for small or micro UAVs weighing only 16.7 grams (modem and GPS receiver not included), shown in Fig. 3. The specifications are shown in Table 2. Kestrel 2.2 includes a complete inertial sensor set including: 3-axis accelerometers, 3-axis angular rate sensors, 2-axis magnetometers, one static pressure sensor (altitude) and one dynamic pressure sensor (airspeed). With the special temperature compensations for sensors, it can estimate the UAV attitude (ϕ and θ) and the wind speed pretty accurately (Beard et al., 2005).

Fig. 3. Procerus Kestrel Autopilot (Beard et al., 2005).

Kestrel has a 29MHz Rabbit 3000 onboard processor with 512K RAM for onboard data logging. It has the built-in ability for autonomous take-off and landing, waypoint navigation, speed and altitude hold. The flight control algorithm is based on the traditional PID control. The autopilot has elevator controller, throttle controller and aileron controller separately. Elevator control is used for longitude and airspeed stability of the UAV. Throttle control is for controlling airspeed during level flight. Aileron control is used for lateral stability of the UAV (Beard et al., 2005). Procerus provides in-flight PID gain tuning with real-time performance graph. The preflight sensor checking and failsafe protections are also integrated to the autopilot software package. Multiple UAV functions are also supported by Kestrel.

2.3.2 Cloud Cap Piccolo

Piccolo family of UAV autopilots from Cloud Cap Company provide several packages for different applications. PiccoloPlus is a full featured autopilot for fixed-wing UAVs. Piccolo *II* is an autopilot with user payload interface added. Piccolo LT is a size optimized one for small electric UAVs as shown in Fig. 4. It includes inertial and air data sensors, GPS, processing, RF data link, and flight termination, all in a shielded enclosure (CloudCap Inc., Accessed 2008). The sensor package includes three gyros and accelerometers, one dynamic pressure sensor and one barometric pressure sensor. Piccolo has special sensor configuration sections to correct errors like IMU to GPS antenna offset, avionics orientation with respect to the UAV body frame.
Piccolo LT has a 40M Hz MPC555 onboard microcontroller. Piccolo provides a universal controller with different user configurations including legacy fixed wing controller, neutral net helicopter controller, fixed wing generation 2 controller, and PID helicopter controller. Fixed

Fig. 4. PICCOLO LT Autopilot (CloudCap Inc., Accessed 2008).

wing generation 2 controller is the most commonly used flight controller for conventional fixed wing UAVs. It includes support for altitude, bank, flaps, heading & vertical rate hold, and auto take-off and landing. Piccolo autopilot supports one ground station controlling multiple autopilots and it also has a hardware-in-the-loop simulation.

2.3.3 Paparazzi Autopilot

Paprazzi autopilot is a pretty popular project first developed by researchers from ENAC university, France. Infrared sensors combined with GPS are used as the default sensing unit. Although Infrared sensors can only provide a rough estimation of the attitude, it is enough for a steady flight control once tuned well. Tiny 13 is the autopilot hardware with the GPS receiver integrated, shown in Fig. 5. Paparazzi also has Tiny Twog autopilot with two open serial ports, which could be used to connect with IMU and modem. One Kalman filter is running on the autopilot to provide a faster position estimation based on GPS updates.

(a) Tiny 13

(b) Paparazzi GCS

Fig. 5. Paparazzi Autopilot System(Brisset et al., 2006).

Paparazzi uses LPC 2148 ARM7 chip as the central processor. For the software, it could achieve waypoints tracking, auto-takeoff & landing, and altitude hold. The flight controller could also be configured if gyro rate is used for roll and pitch tracking control especially for micro UAVs. However, paparazzi doesnt have a good speed hold and changing function currently since no air speed sensor reading is considered in the controller part. Paparazzi is also a truly autonomous autopilot without any rely on the ground control station (GCS). It also has a lot of safety considerations in conditions like RC signal lost, out of predefined range, GPS lost, etc.

2.3.4 Specification Comparisons

The physical specifications of the autopilots are important since small UAVs demand as fewer space, payload and power as possible. The size, weight, and power consumption issues are

shown in Table 2. Both the Crossbow MNAV and Procerus Kestrel have a bias compensation to correct the inertial sensor measurement under different temperatures. The functional specifications of these three typical autopilot are listed in detail in Table 3.

	Size (cm)	Weight (g) w/o radio	Power Consumption	Price (k USD)	DC In (V)	CPU	Memory (K)
Kestrel 2.2	5.08*3.5*1.2	16.7	500mA (3.3 or 5V)	5	6-16.5	29MHz	512
Piccolo LT (w.modem)	11.94*5.72*1.78	45	5W	-	4.8-24	40MHz	448
Pprz Twog	4.02*3.05*1	8	N/A	0.125	6.1-18	32 bit ARM7	512

Table 2. Comparison of Physical Specifications of Autopilots (Chao et al., 2009)

	Kestrel	Picocolo LT	Paparazzi
Waypints Navigation	Y	Y	Y
Auto-takeoff & landing	Y	Y	Y
Altitude Hold	Y	Y	Y
Air Speed Hold	Y	Y	N
Multi-UAV Support	Y	Y	Y
Attitude Control Loop	-	-	20/60 Hz
Servo Control Rate	-	-	20/60 Hz
Telemetry Rate	-	25Hz or faster	Configurable
Onboard Log Rate	$\leq$100Hz	-	N

Table 3. Comparison of Autopilot Functions (Chao et al., 2009)

3. AggieAir UAS Platform

Although most current autopilot systems for UAVs have the ability to autonomously navigate through waypoints, it is actually not enough for the real remote sensing applications since the end users need aerial images with certain spatial and temporal resolution requirements from different bands of cameras. More importantly, most civilian remote sensing users want the UAV platform to be inexpensive. AggieAir UAS platform is developed considering all these remote sensing requirements. AggieAir is a small and low-cost UAV remote sensing platform, which includes the flying-wing airframe, the OSAM-Paparazzi autopilot, the GhostFoto image capture subsystem, the Paparazzi ground control station (GCS), and the gRAID software for aerial image processing. All the subsystems are introduced in detail in this section together with a method to help improve the orthorectification accuracy and calibrate the aircraft sensors using ground references.

3.1 Remote Sensing Requirements

Let $\Omega \subset R^2$ be a polytope including the interior, which can be either convex or nonconvex. A series of band density functions $\eta_{rgb}, \eta_{nir}, \eta_{mir} \ldots$ are defined as $\eta_i(q,t) \in [0,\infty)\ \forall q \in \Omega$. η_{rgb} can also be treated as three bands η_r, η_g, η_b, which represent RED, GREEN and BLUE band values of a pixel. The goal of remote sensing is to make a mapping from Ω to $\eta_1, \eta_2, \eta_3 \ldots$ with a preset spatial and temporal resolution for any $q \in \Omega$ and any $t \in [t_1, t_2]$ (Chao et al., 2008).

With the above remote sensing requirements, several specific characteristics need to be considered to get accurate georeferenced aerial images aside from an autonomous flying vehicle:

- Expense: most civilian applications require inexpensive UAS platforms instead of expensive military unmanned vehicles. However, most commercial-off-the-shelf (COTS) autopilots cost more than $6000, let alone the camera and the air frame.
- Orientation Data: the orientation information when the image is taken is critical to the image georeferencing. But many open source UAS autopilot systems don't have good supports to the accurate sensors. For example, Paparazzi uses IR sensors as the main sensing unit by default.
- Image Synchronization: some COTS UAV could send videos down to the base station and record them on the ground computer. But there is a problem that the picture may not match up perfectly with the UAV data on the data log. The images may not synchronize perfectly with the orientation data from the autopilot.
- Band configurable ability: a lot of remote sensing applications require more than one band of aerial images like vegetation mapping and some of them may require RGB, NIR and thermal images simultaneously.

3.2 AggieAir System Structure

AggieAir UAS includes the following subsystems:

(1) The flying-wing airframe: Unicorn wings with optional 48″, 60″ and 72″ wingspans are used as the frame bed to fit in all the electronic parts. The control inputs include elevons and a throttle motor.

(2) The OSAM-Paparazzi autopilot: the open source Paparazzi autopilot is modified by replacing the IR sensors with the IMU as the main sensing unit. Advanced navigation routines like the survey of a random polygon are also added to support image acquisition of an area with a more general shape.

(3) The GhostFoto imaging payload subsystem: a high resolution camera system with both the RGB and NIR band is developed. More importantly, the image system could guarantee an accurate synchronization with the current autopilot software.

(4) The communication subsystem: AggieAir has a 900MHz data link for GCS monitoring, a 72MHz RC link for safety pilot backup, and an optional 2.4GHz wifi link for real time image transmission.

(5) The Paparazzi ground control station (GCS): Paparazzi open source ground station is used for the real-time UAS health monitoring and flight supervising.

(6) The gRAID software: a new World Wind plug-in named gRAID is developed for aerial image processing including correcting, georeferencing and displaying the images on a 3D map of the world.

The physical structure of AggieAir is shown in Fig. 6, with the specifications in Tab 4 and the airborne layout in Fig. 7.

AggieAir has the following advantages over other UAS platforms for remote sensing missions:

(1) Low costs: AggieAir airborne vehicles are built from scratches including the airframes and all the onboard electronics. The total hardware cost is around $3500.

Fig. 6. AggieAir UAS Physical Structure.

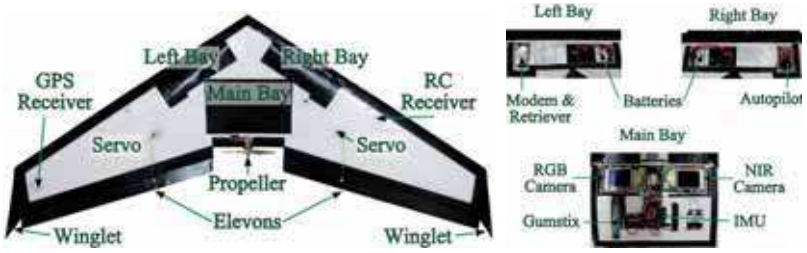

(a) Aircraft Layout (b) Main Bay Layout

Fig. 7. AggieAir UAS Airborne Layout.

	Specifications
Weight	up to 8 lbs
Wingspan	72″
Flight Time	$\leq$ 1 hour
Cruise Sped	15 m/s
Imaging Payload	RGB/NIR/thermal camera
Operational Range	up to 5 miles

Table 4. AggieAir UAS Specifications

(2) Full autonomy: AggieAir uses the Paparazzi autopilot, which supports the total autonomy of the air vehicle even without the ground station.

(3) Easy manipulation: only two people are required to launch, manipulate and land the vehicle.

(4) Run-way free capability: the bungee launching system supports take-off and landing basically at any soft field with only one launching operator.

(5) High spatial and temporal resolution: the image system could achieve submeter level ground resolution and hour level time accuracy.

(6) Multiple bands for cameras: AggieAir supports RGB, and NIR bands for current image subsystems. More band configurable imagers are also under developments.

3.3 OSAM-Paparazzi Autopilot Subsystem

It is clear that Kestrel and Piccolo autopilots are small, light and powerful. But their prices are relatively high and most of their onboard software is not accessible to users, which is a main disadvantage when georeferencing the aerial image after the flight (Jensen et al., 2008). Paparazzi UAV project provides a cheap, robust and open source autopilot solution including both hardware and software. But it uses Infra-red sensors for the attitude measurement, which is not accurate enough when compared with most commercial UAV autopilots above.
To achieve an accurate image georeferencing with a fair price, our team choose to add an inertial measurement unit (IMU) to the Paparazzi autopilot replacing the IR sensors. Paparazzi Tiny WithOut GPS (TWOG) board is used together with the 900MHz Maxtream data modem for real time communication to the GCS. Microstrain Gx2 IMU and Ublox Lea-5H GPS module serve as the attitude and position sensors, respectively. Due to the limits from the IO ports, the gumstix microprocessor is used as a bridge to connect IMU and GPS to the TWOG board. The cascaded PID flight controller then converts all the sensor information into PWM signals for the elevon and throttle motor to guide the vehicle for preplanned navigation. There is also a $72MHz$ RC receiver on board so that the human safety pilot could serve as the backup for the autopilot in case of extreme conditions like strong winds. The physical layout of the airborne system is shown in Fig. 8.

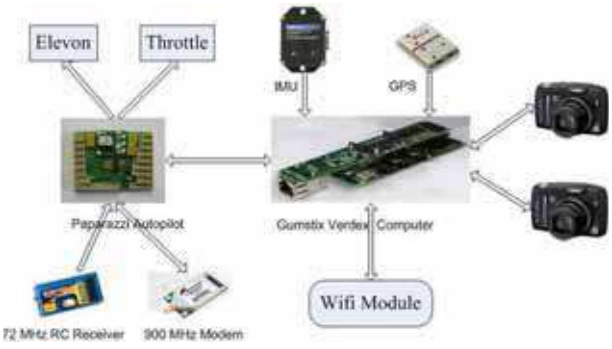

Fig. 8. AggieAir Airborne System Structure.

3.4 GhostFoto Image Subsystem

GhostFoto image subsystem is the second generation remote controlled digital camera system developed at CSOIS (Han, Jensen & Dou, 2009). The hardware includes the Canon CCD camera for image capture and the gumstix microprocessor for payload control and georeferencing logging. Canon PowerShot SX100 IS CCD camera is used, illustrated in Fig. 9. This camera has the remote capturing capability, an 8 mega pixel CCD panel supporting up to 3264 x 2448 pixels size and a $10x$ optical zoom lens with optical image stabilizer. The compact size and relatively light weight ($265g$) of this camera make it easy to fit on small UAVs. Besides the

Fig. 9. Camera Body (left) and its CCD Sensor (right).

commonly used RGB channels, the camera could also support near infrared spectra by replacing the visible light filter with an NIR filter. Our 72" airframe can carry two or three of these imagers with different bands after removing unnecessary parts.
GFoto cameras are remotely controlled by the gumstix through USB 1.1 interface with GhostEye image capture software. GhostEye is based on *libgphoto2* (gPhoto, Accessed 2008), which is an open source portable digital camera library of C functions for UNIX-like operating systems. With *libgphoto2* library functions, GhostEye is able to remotely control and configure multiple cameras simultaneously through a Picture Transfer Protocol (PTP) driver. PTP is a widely supported protocol developed by the International Imaging Industry Association for transfer of images from digital cameras to computers (Picture Transfer Protocol, Accessed 2008). GhostEye also provides the communication link between the payload and the UAV system. Messages can be reported from GhostEye to the ground station. The messages can be shared even with other UAVs with the same protocol. Meanwhile, messages from the UAV system can trigger the imagers. For example, after the altitude of the aircraft reaches a certain level, the plane is able to command the imager to activate or deactivate capturing. The georeferencing data is logged by GhostEye in XML format to import the images into the gRAID.

3.5 gRAID Image Georeference Subsystem

The Geospatial Real-Time Aerial Image Display (gRAID) is a plug-in for NASA World Wind, a 3D interactive open source world viewer (Jensen, 2009). gRAID takes the raw aerial images, makes corrections for the camera radial distortion, and then overlays the images on the 3D earth based upon the position and orientation data collected when they are captured. This process can be done either in real-time while the plane is flying or after the flight. Human-in-the-loop feature based image stitching can be done with conventional GIS software after gRAID exports the image to a world file. gRAID could also create a gray scale image from a single RGB channel. The images can be converted into world files and loaded into conventional GIS software for further, advanced image processing. The detailed georeferecing procedure is described as below.
To georeference the aerial images, several coordinate systems must first be defined, shown in Figure 10.

- The body frame: the origin is defined at the center of gravity (CG), with the x axis pointing through the nose, the y axis pointing to the right wing and the z axis pointing down.
- The camera frame: the origin is located at the focal point of the camera. The axes of the camera frame are rotated by ϕ_c, θ_c and ψ_c with respect to the body frame.
- The inertial frame: the origin is usually defined on the ground with the x, y, z axes pointing towards the north, east and down, respectively. The orientation of the UAV with respect to the NED frame is given by ϕ, θ and ψ.
- The earth centered earth fixed (ECEF) frame: the z axis passes through the north pole, the x axis passes through the equator at the prime meridian and the y axis passes through the equator at 90° longitude.

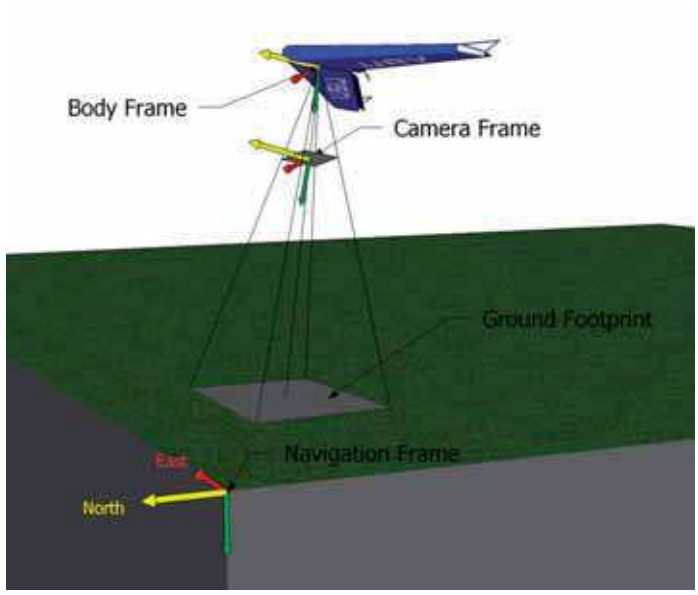

Fig. 10. Aircraft Coordinate Systems

Any point in an image can be rotated from the camera frame to the ECEF coordinate system in order to find where it is located on the earth. However, it is only necessary to find the location of the four corners of the image in order to georeference it. Assuming the origin is at the focal point and the image is on the image plane, equation 1 can be used to find the four corners of the image. As defined in figure 11, FOV_x is the FOV around the x axis, FOV_y is the FOV around the y axis and f is the focal length.

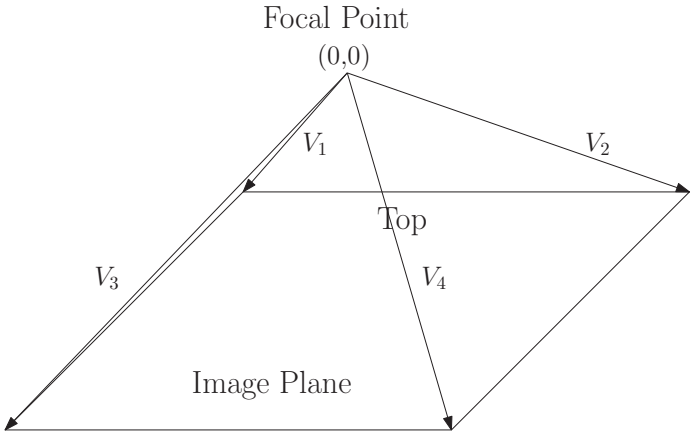

Fig. 11. Definition of Initial Image Corners

$$v_c^1 = \begin{bmatrix} f\tan(FOV_y/2) & -f\tan(FOV_x/2) & f \end{bmatrix} \quad (1)$$

$$v_c^2 = \begin{bmatrix} f\tan(FOV_y/2) & f\tan(FOV_x/2) & f \end{bmatrix} \quad (2)$$

$$v_c^3 = \begin{bmatrix} -f\tan(FOV_y/2) & -f\tan(FOV_x/2) & f \end{bmatrix} \quad (3)$$

$$v_c^4 = \begin{bmatrix} -f\tan(FOV_y/2) & f\tan(FOV_x/2) & f \end{bmatrix} \quad (4)$$

To rotate the corners into the navigation frame, they first need to be rotated into the body frame. The Euler angles with respect to the body frame are given by ϕ_c, θ_c and ψ_c, and can be used to create a clock-wise rotation matrix R_c^b which rotates a vector in the body frame to the camera frame.

$$R_c^b = R_{xyz}(\phi_c, \theta_c, \psi_c) \quad (5)$$

To rotate from the camera frame to the body frame, the transpose of R_c^b is used.

$$R_b^c = (R_c^b)^T = R_{zyx}(-\theta_c, -\psi_c, -\phi_c) \quad (6)$$

The same rotation matrix is used, with ϕ, θ and ψ, to rotate from the body into the navigation frame.

$$R_n^b = (R_b^n)^T = R_{zyx}(-\theta, -\psi, -\phi) \quad (7)$$

Now each corner is rotated from the camera frame into the navigation frame using equation 8.

$$v_n^i = R_n^b R_b^c v_c^i \quad (8)$$

Now that the corners are in the NED coordinate system, they are scaled to the ground to find their appropriate magnitude (assuming flat earth) where h is the height of the UAV above ground and $v_n^i(z)$ is the z component of v_n^i.

$$v_n^i = v_n^i \frac{h}{v_n^i(z)} \tag{9}$$

The next step is to rotate the image corners into the ECEF coordinate system. This is done with another rotation matrix and the latitude (λ) and longitude (α) of the UAV.

$$R_w^n = R_{zyy}(-\alpha, \frac{\pi}{2}, \lambda) \tag{10}$$

$$v_w^i = R_w^n v_n^i \tag{11}$$

After the corners are rotated into the ECEF coordinate system, they are located in the center of the earth and need to be translated up to the position of the UAV in cartesian coordinates (p).

$$v_w^i = v_w^i + p \tag{12}$$

Now v_w^i represents the position of each of the image corners, in cartesian coordinates, projected on the earth.

3.6 Image Orthorectification

Even though small, low-cost unmanned aerial vehicles (UAVs) make good remote sensing platforms by reducing the cost and making imagery easier to obtain, there are also some tradeoffs. The low altitude, small image footprint and high number of images make it difficult and tedious to georeference the images based on features. Auto-orthorectification techniques based on the position and attitude of the UAV would work well except the inherent errors in the UAV sensors reduce the accuracy of the orthorectification significantly. The orthorectification accuracy can be improved by calibrating the UAV sensors. This is done by inverse orthorectifing the images to find the actual position and attitude of the UAV using ground references setup in a square. Actual data from a test flight is used to validate this method (Jensen, Han & Chen, 2009).

As detailed above, a point in the image plane ($\vec{p_i}$) can be transformed into Earth-Centered Earth-Fixed (ECEF) coordinates ($\vec{p_w}$) using equation 13 where $\vec{u_w}$ is the position of the UAV in ECEF, R_b^c is the rotation matrix from the camera frame to the body frame, R_n^b is the rotation matrix from the body frame to the navigation frame, R_w^n is the rotation matrix from the navigation frame to ECEF, and h is the height above ground of the UAV.

$$\vec{p_w} = aR_w^n R_n^b R_b^c \vec{p_i} + \vec{u_w} \tag{13}$$

$$a = \frac{h}{\vec{v_z}^T R_n^b R_b^c \vec{p_i}}$$

$$\vec{v_z} = \begin{bmatrix} 0 \\ 0 \\ 1 \end{bmatrix}$$

There is a possibility that equation 13 could be used directly to find the position and attitude of the UAV given multiple known ground control points ($\vec{p_w}$) and their positions on an image ($\vec{p_i}$). However, this could prove to be very complicated. The method presented here will take a simple, indirect approach by setting up the ground control points in a square (Figure 12). The

properties of this square, where the locations of the corners are measured, can be compared to the properties of another square where the corner positions are estimated using equation 13. By changing the position and attitude of the UAV, the properties of the estimated square can be adjusted to match the properties of the measured square. The correct position and attitude of the UAV is found when the properties of the measured and estimated squares match. For example, the difference between the areas of each square reflects the measured and actual altitude of the UAV above ground. If the measured square has an area greater than the area of the estimated square, the altitude of the UAV needs to be increased. The estimated square is then recalculated using equation 13 and the areas are compared again. Once the areas match, the correct altitude is found.

Fig. 12. Ground Targets in Square

The position and yaw of the UAV are easier to find than the altitude. This is because the difference in the position and orientation of the squares are directly related to the difference between the measured and actual position and yaw of the UAV. Therefore, the difference between the position and orientation of the squares can simply be added to the measured values of the position and yaw of the UAV to find the actual position and yaw.
Finding a property of the square related to roll and pitch is more complicated than the other properties. The shape, the length of each side and the length of the diagonals could all have a relationship to roll and pitch. However, this relationship all depends on the orientation of the square relative to the image. More work will need to be done in order to find the actual roll and pitch with this method.
This method was tested by collecting 40 images of the ground references at various heights and headings. Without any correction, the position of the ground references had errors of up to 45m. Correcting the altitude did not show significant improvement, however correcting the yaw decreased the error to below 20m. Correcting for the position also had a profound effect and reduced the error to below 5m of error.

Linear relationships were also found between the actual and measured position and attitude of the UAV from the experiment. The altitude had a small bias of 4m and a slope of 0.93 which shows that the error of the altitude gets worse as the altitude increases. The yaw was also very linear with a one-to-one relationship and a bias of 13 degrees. A relationship between the actual and measured position was more unclear but still showed that as the altitude increases, the magnitude of the position error also increases. The unclear relationship in the position error is probably because the roll and pitch were not compensated for. The direction of the position error, however, had a linear relationship with the heading of the aircraft with a bias of 64 degrees. This could be due to a misalignment between the cameras and the body axis of the aircraft.

4. Sample Applications for AggieAir

The typical sample application of using the AggieAir UAS for remote sensing missions could be defined as follows (Chao et al., 2008). Given a random area Ω, UAVs with functions of altitude and speed maintenance and waypoint navigation: speed $v \in [v_1, v_2]$, possible flight height $h \in [h_1, h_2]$, camera with specification: focal length F, image sensor pixel size: $PS_h \times PS_v$, image sensor pixel pitch $PP_h \times PP_v$, the interval between images acquired by the camera (the "camera shooting interval") t_{shoot}, the minimal shooting time $t_{shoot_{min}}$, the desired aerial image resolution res, the control objective is:

$$\min t_{flight} = g(\Omega, h, v, \{q_1, \ldots, q_i\}, t_{shoot}, res), \tag{14}$$

$s.t. v \in [v_1, v_2], h \in [h_1, h_2], t_{shoot} = k \times t_{shoot_{min}}$. where t_{flight} is the flight time of the UAV for effective coverage, $g(\Omega, h, v, t_{shoot})$ is the function to determine the flight path and flight time for effective coverage, k is a positive integer. In other words, the UAS is required to make a full coverage map of the given area, which could also be called the coverage control problem. The control inputs of the coverage controller include bounded velocity v, bounded flight height H, a set of preset UAV waypoints $\{q_1, q_2, \ldots, q_i\}$ and the camera shooting interval t_{shoot}. The system states are the real UAV trajectory $\{\bar{q}_{t_1}, \ldots, \bar{q}_{t_2}\}$ and the system output is a series of aerial images or a video stream taken between t_1 and t_2.
Assume the imager is mounted with its lens vertically pointing down towards the earth; its footprint (shown in Fig. 13) can be calculated as:

$$FP_h = \frac{h \times PP_h \times PS_h}{F}, FP_v = \frac{h \times PP_v \times PS_v}{F}.$$

Most UAVs can maintain a certain altitude while taking pictures so the UAV flight height h can be determined first based on camera and resolution requirements. Assuming that different flight altitudes have no effect on the flight speed, we get

$$h = \frac{\sqrt{res} \times F}{max(PP_h, PP_v)}. \tag{15}$$

Given the flight height h and the area of interest Ω, the flight path, cruise speed and camera shooting interval must also to be determined. Without loss of generality, Ω is assumed to be a rectangular since most other polygons can be approximated by several smaller rectangles. The most intuitive flight path for the UAV flight can be obtained by dividing the area into strips based on the group spatial resolution, shown in Fig. 14(a). The images taken during

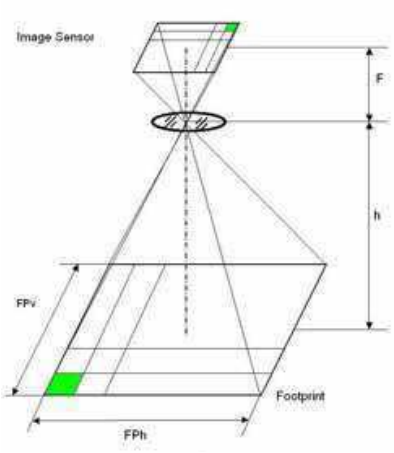

Fig. 13. Footprint Calculation.

UAV turning are not usable because they may have bad resolutions. Due to the limitation from the autopilot, GPS accuracy and wind, the UAV cannot fly perfectly straight along the preset waypoints. To compensate the overlapping percentage between two adjacent sweeps o must also be determined before flight; this compensation is based on experience from the later image stitching as shown in Fig. 14(b).

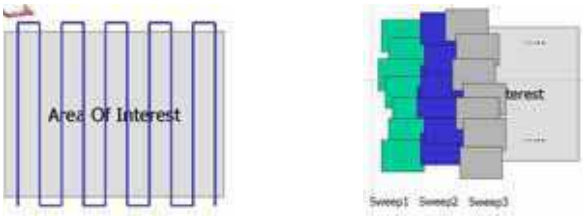

(a) Ideal Flight Path (b) Flight Path with Overlap

Fig. 14. UAV Flight Path.

Given the overlapping percentage $o\%$ between sweeps, the ground overlapping o_g can be determined by:

$$o_g = (1 - o\%) \times FP_h. \tag{16}$$

The minimal camera shooting interval can be computed as:

$$t_{shoot_{min}} = \frac{(1 - o\%) \times FP_v}{v}. \tag{17}$$

This open-loop solution is intuitive, robust to all the polygons and requires little computation. However, this method requires that many parameters, especially the overlapping percentage

o% to be set up based on experience; it cannot provide an optimal solution. More work on a close-loop real-time solution is needed for an optimal solution.
Preliminary experimental results are shown in this section to demonstrate the effectiveness of the whole UAV remote sensing system on both the hardware and software levels. Three sample applications are introduced in detail. A remote data collection application is offered to demonstrate the feasibility of using UAVs to collect data from ground-based sensors through wireless modems. Acquisition of photographic data over Desert Lake, Utah, illustrates an application involving the use of the RGB and NIR imagers. The data collected by UAVs from ground sensors can also be used for comparison and calibration with information from UAV images. Finally, we present a farmland coverage test with image stitching in our regular test flight site.

4.1 Farmland Coverage

The goal of irrigation control is to minimize the water consumption while sustaining the agriculture production and human needs (Fedro et al., 1993). This optimization problem requires remote sensing to provide real-time feedback from the farmland field including:

- Water: water quantity and quality with temporal and spatial information, for example water level of a canal or lake.
- Soil: soil moisture and type with temporal and spatial information.
- Vegetation: vegetation index, quantity and quality with temporal and spatial information, for example the stage of growth of the crop.

The "real-time" here means daily or weekly temporal resolution based on different applications. AggieAir is currently involved in a large scale agricultural project which will use visual and NIR images from AggieAir to measure the soil moisture of the area to help save water (Jensen, Chen, Hardy & McKee, 2009). The project includes 30 square miles of different types of crops where 87 wireless soil moisture ground probes are placed. The ground probes sample and send the data every hour through wireless to a base station where the data is displayed on the Internet. The ground probes and Landsat data will be used to calibrate the images from AggieAir using the downscaling techniques described in (Kaheil, Gill, McKee, Bastidas & Rosero, 2008) and (Kaheil, Rosero, Gill, McKee & Bastidas, 2008). After calibration, these images should be able to measure soil moisture and evapotranspiration for water managers and farmers whenever it is needed. However, AggieAir has not yet been flown for this project due to the large area and the high altitude AggieAir will need to fly at. Approval from the Federal Aviation Administration (FAA) is currently being sought to ensure the safety of all airborne vehicles before AggieAir is flown for this project. A research farm (one square mile) coverage map is provided in Fig. 15 to show the capability of AggieAir.

4.2 Road Surveying

AggieAir UAS could also provide low-cost aerial images for road and highway construction and maintenance. Figure 16 shows a highway intersection located in Logan Canyon, which was recently rebuilt for better safety to turn onto the main road. The Utah Department of Transportation (UDOT) usually needs to photograph the area to be built or altered before construction with a manned aircraft. However no imagery is available during or after construction due to the cost and availability of the imagery. UDOT is not only interested in AggieAir to lower the cost and increase the availability of imagery for construction, but also to update their inventory of signs, culverts, traffic lines, etc. The aerial images acquired by manned aircraft and by AggieAir are shown in Fig. 16.

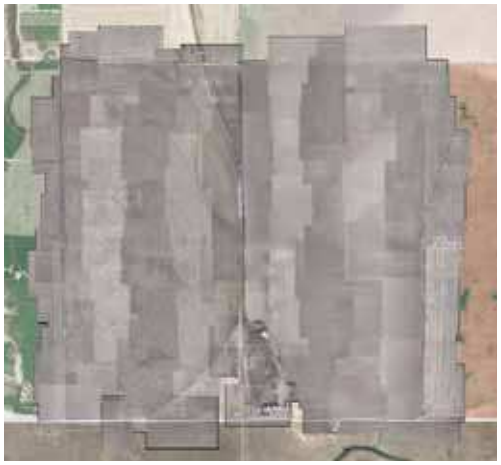

Fig. 15. Cache Junction Farm Coverage Map

(a) Before Construction (b) After Construction (AggieAir)

Fig. 16. Beaver Resort Intersection

4.3 Water Area Coverage

Water areas include wetlands, lakes, or ponds, etc. Water areas could provide lots of information to ecological environment changes, flood damage predictions, and water balance management. Desert Lake coverage mission is a typical example, which lies in west-central Utah (latitude: $39°22'5''N$, longitude: $110°46'52''W$). It is formed from return flows from irrigated farms in that area. It is also a waterfowl management area. This proposes a potential problem because the irrigation return flows can cause the lake to have high concentrations of mineral salts, which can affect the waterfowl that utilize the lake. Managers of the Desert Lake resource are interested in the affect of salinity control measures that have been recently constructed by irrigators in the area. This requires estimation of evaporation rates from the Desert Lake area, including differential rates from open water, wetland areas, and dry areas. Estimation of these rates requires data on areas of open water, wetland, and dry lands, which, due to the relatively small size and complicated geometry of the ponds and wetlands of Desert Lake, are not available from satellite images. A UAV can provide a better solution for the problem of acquiring periodic information about areas of open water, etc., since it can be flown more frequently and at little cost.

The whole Desert Lake area is about $2 * 2$ miles. It is comprised of four ponds and some wetland areas. The early version of AggieAir imaging payload, GFDV, is used in this mission together with the Procerus UAV with real-time, simultaneous RGB and NIR videos. Both the RGB and NIR videos are transmitted back to the ground station in real time. The photos are stitched using gRAID, shown in Fig 17.

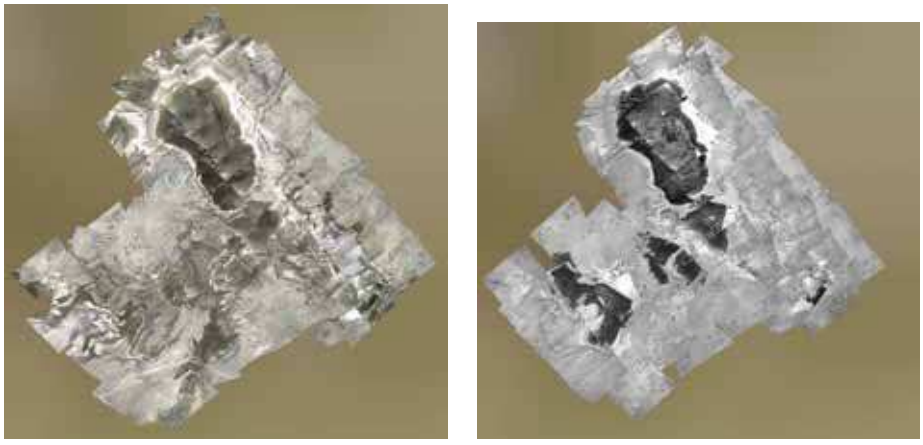

(a) RGB Image (b) NIR Image

Fig. 17. Desert Lake Coverage Map

4.4 Riparian Surveillance

Riparian buffer surveillance is becoming increasingly more important since it is challenging to maintain stream ecosystem integrity and water quality with the current rapidly changing land use (Goetz, 2006). AggieAir UAS could be used in several applications including river tracking, vegetation mapping and hydraulic modeling, etc.

4.4.1 River Tracking

The path and flow of a river might constantly change due to drought, flood or other natural calamities. Because of this, the aerial images of the river path could be outdated or in low quality, making it difficult to perform studies of the changed river and the variations of its nearby ecological system. AggieAir UAS platform with the high resolution multi-spectral camera system could present a real-time low-cost solution to the river tracking problem Han, Dou & Chen (2009). A flight plan with 3D waypoints could be formed by integrating flow line data from NHDPlus (National Hydrography Dataset Plus) and DEM (Digital Elevation Model) from USGS (U.S. Geological Survey). The images captured by the cameras are processed in real time. Based on the information derived from these images, waypoints are dynamically generated for the autonomous navigation so that the UAV can exactly follow the changed river path and the focus of each image from the camera system is on the center of the river. The actual flight results collected in several flying experiments along a river verify the effectiveness of AggieAir System, shown in Fig 18. Example RGB and NIR pictures acquired by AggieAir is also shown in Fig 19.

Fig. 18. River Tracking Map after Stitching.

4.4.2 Vegetation Mapping & Hydraulic Modeling

Figure 20 shows some imagery taken with AggieAir of a small section of the Oneida Narrows near Preston Idaho. A team of engineers used this imagery to map the substrate and vegetation for 2D hydraulic and habitat modeling. Normally, the team uses low resolution, outdated imagery to map rivers. This can be difficult when the vegetation, the path and the flow of the river are always changing. The imagery from AggieAir, however, was up-to-date (within a week) and had high resolution (5 cm), which made mapping the river quick and easy. Not only could different types of vegetation be distinguished from the imagery, but different types of sediment, like sand piles, could also easily be distinguished.

4.5 Remote Data Collection

Many agricultural and environmental applications require deployment of sensors for measurement of the interested field. However, it is not always easy or inexpensive to collect all

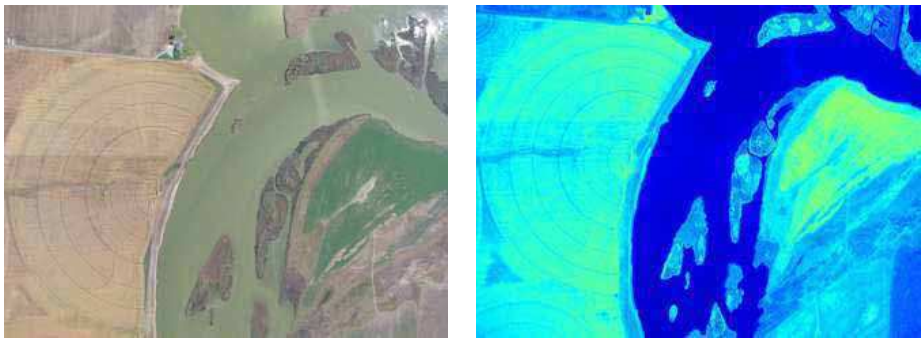

(a) RGB Image (b) NIR Image

Fig. 19. Sample Picture for River Tracking

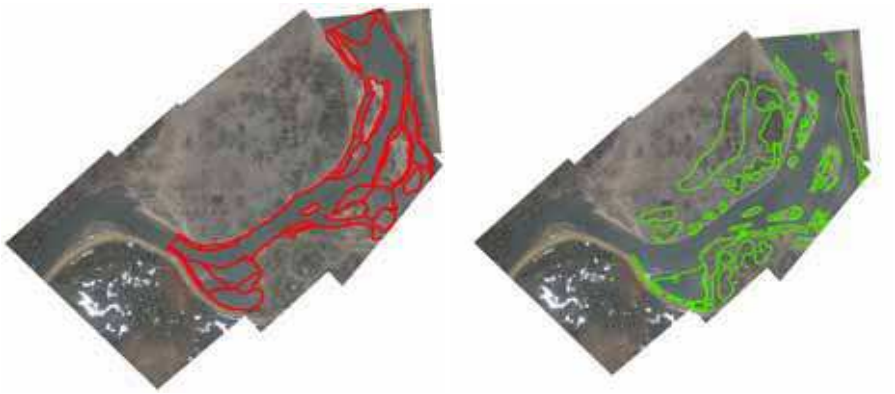

(a) Substrate Map (b) Vegetation Map

Fig. 20. Oneida Narrows Imagery

the data from remote data loggers for further processing. Many applications still require humans to get close to the ground-based sensors to retrieve the data from their data loggers. Wireless sensor networks and satellite networks are used in environmental data collection applications, but wireless communication can be expensive and vulnerable to changing environmental conditions (such as loss of line-of-sight due to vegetation growth). This problem is especially difficult when the sensors are deployed sparsely over a large geographic area where transportation might be limited by terrain conditions. UAVs can fly into such areas without affecting the vegetation on the ground; they can spare humans from having to enter dangerous or difficult areas; and they might be able to operate at lower costs that might be required for approaches involving direct human access to the data. Moreover, UAVs can achieve better wireless communication since the signal can be transmitted more dependably in the air than near ground level.

One typical example of remote data collection is fish tracking. In order to understand fish habitats, radio transmitters are planted in fish in order to locate and track their movements. Human operators are needed to drive a boat around a lake or down a river following the periodic beacon sent from the transmitters. The beacon is heard through a radio receiver with a directional antenna and its strength is highly dependent on the distance and the direction the antenna is pointed at. AggieAir could be employed here with an onboard self-designed device to catch the signal from the transmitter and record its strength. Thus, the location of the fish can be found and recorded much easier and faster since the wireless signal transmits much better in the air. Hardware developments and real experiments are still undergoing.

5. Towards Band Reconfigurable Multiple UAV based Remote Sensing

A single AggieAir system could have many applications as mentioned above, but some irrigation applications may require remote sensing of a large land area (more than 30 square miles) within a short time (less than one hour). Acquisition of imagery on this geographic scale is difficult for a single UAV. However, groups of UAVs (which we call "covens") can solve this problem because they can provide images from more spectral bands in a shorter time than a single UAV.
The following missions will need multiple UAVs (covens) operating cooperatively for remote sensing:

- Measure $\eta_1, \eta_2, \eta_3 \ldots$ simultaneously.
- Measure $\eta_i(q,t)$ within a short time.

To fulfill the above requirements, UAVs equipped with imagers having different wavelength bands must fly in some formation to acquire the largest number of images simultaneously. The reason for this requirement is that electromagnetic radiation may change significantly, even over a period of minutes, which in turn may affect the final product of remote sensing. The "V" or "—" formation, keeping algorithm similar to the axial alignment (Ren et al., 2008), can be used here since the only difference is that the axis is moving:

$$\dot{q}_m^d = -\sum_{n \in \mathcal{J}_m(t)} [(q_m - q_n) - (\delta_m - \delta_n)], \tag{18}$$

where q_m^d is the preset desired waypoints, $\mathcal{J}_m(t)$ represents the UAV group, $\delta_m = [\delta_{mx}, \delta_{my}]^T$ can be chosen to guarantee that the UAVs align on a horizontal line with a certain distance in between.
Based on the theoretical analysis and our preliminary results, more effort is needed to achieve the final band reconfigurable multi-UAV based cooperative remote sensing.

- (1) Multiple UAVs: the preliminary results have shown that the sensing range of the AggieAir UAS is about 2.5×2.5 miles, given the current battery energy density. However, light reflection varies a great deal in one day and accurate NIR images require at most a one-hour acquisition time for capture of the entire composite image. This motivates the use of covens, or multiple UAVs, for this type of application, with each UAV carrying one imager with a certain band.
- (2) More robust control: the current UAV platform requires winds of less than 10 m/s. However, the UAV needs to have the ability to deal with wind gusts, which is problematic for UAV flight.

- (3) Accurate real-time image stitching and registration: the current software requires manual post processing for accurate georeferencing results. For the application to be attractive to managers of real irrigation systems, manual post processing is unacceptable because of its cost and requirement of technically trained individuals.

Acknowledgement

This work is supported in part by the Utah Water Research Laboratory (UWRL) MLF Seed Grant (2006-2009) on "Development of Inexpensive UAV Capability for High-Resolution Remote Sensing of Land Surface Hydrologic Processes: Evapotranspiration and Soil Moisture." This work is also partly supported by NSF Grants #0552758 and #0851709. The authors would like to thank Professor Raymond L. Cartee for providing the Utah State University research farm at Cache Junction as the UAV flight test field, and Calvin Coopmans, Long Di, Daniel Morgan for their technical support and help to the flight tests. The authors would also like to thank Shannon Clemens for georeferencing and generating mosaics.

6. References

Beard, R., Kingston, D., Quigley, M., Snyder, D., Christiansen, R., Johnson, W., Mclain, T. & Goodrich, M. (2005). Autonomous vehicle technologies for small fixed wing UAVs, *AIAA J. Aerospace Computing, Information, and Communication* **5**(1): 92–108.

Brisset, P., Drouin, A., Gorraz, M., Huard, P. S. & Tyler, J. (2006). The paparazzi solution, *MAV 2006*, Sandestin, Florida, USA.

Calise, A. J., Johnson, E. N., Johnson, M. D., & Corban, J. E. (2003). Applications of adaptive neural-network control to unmanned aerial vehicles, *in Proc. AIAA/ICAS Int. Air and Space Symp. and Exposition: The Next 100 Years*, Dayton, Ohio, USA.

Chao, H., Baumann, M., Jensen, A. M., Chen, Y. Q., Cao, Y., Ren, W. & McKee, M. (2008). Band-reconfigurable multi-UAV-based cooperative remote sensing for real-time water management and distributed irrigation control, *in Proc. IFAC World Congress*, Seoul, Korea, pp. 11744–11749.

Chao, H., Cao, Y. & Chen, Y. Q. (2009). Autopilots for small fixed wing unmanned aerial vehicles: a survey, *Int. J. Control, Automation and Systems* . Accepted to appear.

CloudCap Inc. (Accessed 2008).
URL `http://www.cloudcaptech.com`.

Damien, D., Wageeh, B. & Rodney, W. (2007). Fixed-wing attitude estimation using computer vision based horizon detection, *in Proc. Australian Int. Aerospace Congress*, Melbourne, Australia, pp. 1–19.

Egan, G. K. (2006). The use of infrared sensors for absolute attitude determination of unmanned aerial vehicles, *Tech. Rep. MECSE-22-2006*, Monash University.

Fedro, S. Z., Allen, G. S. & Gary, A. C. (1993). Irrigation system controllers, *Series of the Agricultural and Biological Engineering Department, Florida Cooperative Extension Service, Institute of Food and Agricultural Sciences, University of Florida* .
URL: *http://edis.ifas.ufl.edu/AE077*

Goetz, S. J. (2006). Remote sensing of riparian buffers: Past progress and future prospects, *Journal of the American Water Resources Association* **42**(11): 133–143.

gPhoto (Accessed 2008).
URL `http://www.gphoto.org/`.

Han, Y., Dou, H. & Chen, Y. Q. (2009). Mapping river changes using low cost autonomous unmanned aerial vehicles, *in Proc. AWRA Spring Specialty Conf. Managing Water Resources Development in a Changing Climate*, Anchorage, Alaska, USA.

Han, Y., Jensen, A. M. & Dou, H. (2009). Programmable multispectral imager development as light weight payload for low cost fixed wing unmanned aerial vehicles, *in Proc. ASME Design Engineering Technical Conf. Computers and Information in Engineering*, number MESA-87741, San Diego, California, USA.

James, B. (2006). *Introduction to Remote Sensing*, 4th edn, Guilford Press.

Jensen, A. M. (2009). *gRAID: A geospatial real-time aerial image display for a low-cost autonomous multispectral remote sensing platform*, M.S. Thesis, Utah State Univeristy.

Jensen, A. M., Baumann, M. & Chen, Y. Q. (2008). Low-cost multispectral aerial imaging using autonomous runway-free small flying wing vehicles, *in Proc. IEEE Int. Conf. Geoscience and Remote Sensing Symp.*, Boston, Massachusetts, USA, pp. 506–509.

Jensen, A. M., Chen, Y. Q., Hardy, T. & McKee, M. (2009). AggieAir - a low-cost autonomous multispectral remote sensing platform: New developments and applications, *in Proc. IEEE Int. Conf. Geoscience and Remote Sensing Symp.*, Cape Town, South Africa, pp. –.

Jensen, A. M., Han, Y. & Chen, Y. Q. (2009). Using aerial images to calibrate inertial sensors of a low-cost multispectral autonomous remote sensing platform (AggieAir), *in Proc. IEEE Int. Conf. Geoscience and Remote Sensing Symp.*, Cape Town, South Africa, pp. –.

Johnson, L., Herwitz, S., Dunagan, S., Lobitz, B., Sullivan, D. & Slye, R. (2003). Collection of ultra high spatial and spectral resolution image data over California vineyards with a small UAV, *in Proc. Int. Symp. Remote Sensing of Environment*, Honolulu, Hawai, USA.

Johnson, L., Herwitz, S., Lobitz, B. & Dunagan, S. (2004). Feasibility of monitoring coffee field ripeness with airborne multispectral imagery, *Applied Engineering in Agriculture* **20**: 845–849.

Kaheil, Y. H., Gill, M. K., McKee, M., Bastidas, L. A. & Rosero, E. (2008). Downscaling and assimilation of surface soil moisture using ground truth measurements, *IEEE Trans. Geoscience and Remote Sensing* **46**(5): 1375–1384.

Kaheil, Y. H., Rosero, E., Gill, M. K., McKee, M. & Bastidas, L. A. (2008). Downscaling and forecasting of evapotranspiration using a synthetic model of wavelets and support vector machines, *IEEE Trans. Geoscience and Remote Sensing* **46**(9): 2692–2707.

Microstrain Inc. (Accessed 2008).
URL `http://www.mirostrain.com`.

Paparazzi Forum (Accessed 2008).
URL `http://www.recherche.enac.fr/paparazzi/`.

Picture Transfer Protocol (Accessed 2008).
URL `http://en.wikipedia.org/wiki/Picture_Transfer_Protocol`.

Ren, W., Chao, H., Bourgeous, W., Sorensen, N. & Chen., Y. Q. (2008). Experimental validation of consensus algorithms for multi-vehicle cooperative control, *IEEE Trans. Control Systems Technology* **16**(4): 745–752.

Roberts, P. J., Walker, R. A. & O'Shea, P. J. (2005). Fixed wing UAV navigation and control through integrated GNSS and vision, *in Proc. AIAA Guidance, Navigation, and Control Conf. and Exhibit*, number AIAA 2005-5867, San Francisco, California, USA.

Tarbert, B., Wierzbanowski, T., Chernoff, E. & Egan, P. (2009). Comprehensive set of recommendations for sUAS regulatory development, *Tech. Rep.*, Small UAS Aviation Rulemaking Committee.

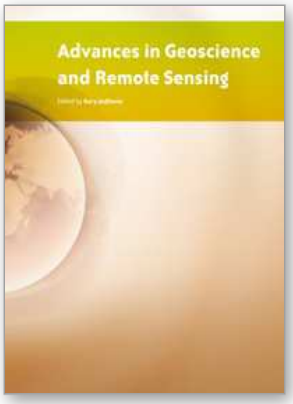

Advances in Geoscience and Remote Sensing

Edited by Gary Jedlovec

ISBN 978-953-307-005-6

Hard cover, 742 pages

Publisher InTech

Published online 01, October, 2009

Published in print edition October, 2009

Remote sensing is the acquisition of information of an object or phenomenon, by the use of either recording or real-time sensing device(s), that is not in physical or intimate contact with the object (such as by way of aircraft, spacecraft, satellite, buoy, or ship). In practice, remote sensing is the stand-off collection through the use of a variety of devices for gathering information on a given object or area. Human existence is dependent on our ability to understand, utilize, manage and maintain the environment we live in - Geoscience is the science that seeks to achieve these goals. This book is a collection of contributions from world-class scientists, engineers and educators engaged in the fields of geoscience and remote sensing.

InTech Europe

University Campus STeP Ri
Slavka Krautzeka 83/A
51000 Rijeka, Croatia
Phone: +385 (51) 770 447
Fax: +385 (51) 686 166
www.intechopen.com

InTech China

Unit 405, Office Block, Hotel Equatorial Shanghai
No.65, Yan An Road (West), Shanghai, 200040, China
中国上海市延安西路65号上海国际贵都大饭店办公楼405单元
Phone: +86-21-62489820
Fax: +86-21-62489821